Synthesis, Biochemical, and Cellular Evaluation of Farnesyl Monophosphate Prodrugs as Farnesyltransferase Inhibitors

Michelle K. Clark,[†,‡] Sarah A. Scott,[†,‡] Jonathan Wojtkowiak,[†,§] Rosemarie Chirco,[∥] Patricia Mathieu,[⊥] John J. Reiners, Jr.,[§,∥,⊥] Raymond R. Mattingly,[§,∥] Richard F. Borch,*[,‡] and Richard A. Gibbs*[,‡]

Medicinal Chemistry and Molecular Pharmacology and Cancer Center, Purdue University, West Lafayette, Indiana 47907, and Pharmacology, Cancer Biology, and Institute of Environmental Health Sciences, Wayne State University, Detroit, Michigan 48202

Received February 16, 2007

Certain farnesyl diphosphate (FPP) analogs are potent inhibitors of the potential anticancer drug target protein farnesyltransferase (FTase), but these compounds are not suitable as drug candidates. Thus, phosphoramidate prodrug derivatives of the monophosphate precursors of FPP-based FTase inhibitors have been synthesized. The monophosphates themselves were significantly more potent inhibitors of FTase than the corresponding FPP analogs. The effects of the prodrug **5b** (a derivative of 3-allylfarnesyl monophosphate) have been evaluated on prenylation of RhoB and on the cell cycle in a human malignant schwannoma cell line (STS-26T). In combination treatments, 1−3 μM **5b** plus 1 μM lovastatin induced a significant inhibition of RhoB prenylation, and a combination of these drugs at 1 μM each also resulted in significant cell cycle arrest in G_1. Indeed, combinations as low as 50 nM lovastatin + 1 μM **5c** or 250 nM lovastatin + 50 nM **5c** were highly cytostatic in STS-26T cell culture.

Introduction

Prenylation (the introduction of a farnesyl (C_{15}) or geranylgeranyl (C_{20}) moiety on the sulfhydryl group of certain proteins) is an important post-translational modification central to many cellular processes. Prenylation is required to give a protein sufficient hydrophobicity to translocate to the plasma membrane. Many of the proteins that undergo prenylation are critical to signal transduction pathways, and cell membrane localization is essential for these proteins to function properly.[1−3] Ras proteins,[4] including the mutant forms that are constitutively activated in a significant number of cancers, require farnesylation and two subsequent modifications for biological activity (Scheme 1). Thus, intense efforts have been focused on inhibiting protein-farnesyltransferase (FTase[a]), the enzyme responsible for protein farnesylation.[5,6] Two FTase inhibitors (**1** (R-115777)[7] and **2** (SCH66336),[8] Scheme 1) have advanced into Phase III clinical trials for the treatment of solid tumors and hematologic malignancies.[6,9] These agents, derived from leads identified through compound library screens for FTase inhibition, block the enzyme in a peptide-competitive manner, as do the majority of reported FTase inhibitors.

Gibbs and colleagues have a longstanding interest in developing FTase inhibitors that mimic farnesyl diphosphate (FPP; **3a**, Scheme 2), which is the natural lipid cosubstrate for the enzyme.[5] The diphosphates of 3-allylfarnesol (**3b**, Scheme 2), 3-*tert*-butylfarnesol (**3c**, Scheme 2), and several other FPP analogs are nanomolar inhibitors of FTase.[10,11] The diphosphates

Scheme 1

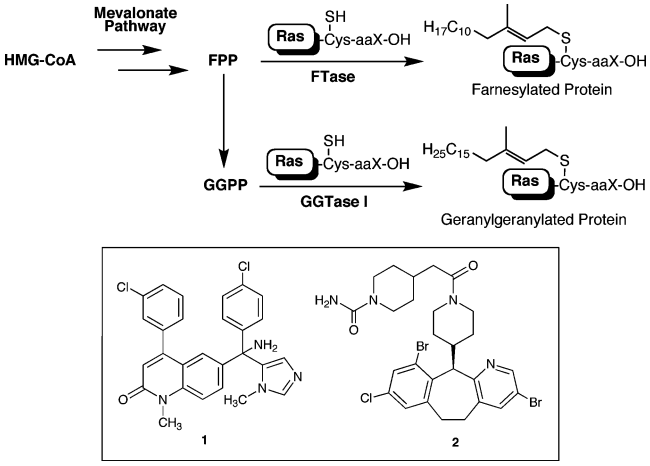

are highly charged and easily hydrolyzed, however, and, thus, they do not appear to be viable drug candidates. We have previously demonstrated that 3-allylfarnesol (**4b**, Scheme 2) is a potent inhibitor of prenylation in cells, particularly in combination with lovastatin.[10] Presumably, **4b** is converted into the corresponding FPP analog **3b** through the farnesol salvage pathway.[12] However, despite efficacy in NIH-3T3 fibroblasts,[10] A10 vascular smooth muscle cells,[13] cultured pancreatic beta cells,[14] and certain tumor cell types (unpublished results), there are other cell types where 3-allylfarnesol was completely ineffective. Moreover, this approach is only effective with 3-allylfarnesol and certain other selected analogs; 3-*tert*-butylfarnesol (**4c**) is completely inactive in NIH-3T3 cells,[10] despite the fact that the corresponding diphosphate (**3c**) is a more potent FTase inhibitor than 3-allylFPP (**3b**). Presumably, both of these problems result from inefficient intracellular conversion of the farnesol precursors to the active diphosphate inhibitors via the isoprenoid salvage pathway[12] due either to a lack of the required isoprenoid kinase(s) (in the former case) or its restricted substrate specificity (in the latter case). This is unfortunate, as FPP-competitive FTase inhibitors may have

* To whom correspondence should be addressed. Tel.: 765-494-1456 (R.A.G.); 765-494-1403 (R.F.B.). Fax: 765-494-1414 (R.A.G.; R.F.B.). E-mail: rag@pharmacy.purdue.edu (R.A.G.); rickb@pharmacy.purdue.edu (R.F.B.).

† These three authors contributed equally to the work described in this manuscript.

‡ Purdue University.

§ Pharmacology, Wayne State University.

∥ Cancer Biology, Wayne State University.

⊥ Institute of Environmental Health Sciences, Wayne State University.

[a] Abbreviations: FPP, farnesyl diphosphate; FTase, protein farnesyltransferase; STS-26T, human malignant schwannoma cell line; SDS-PAGE, sodium dodecyl sulfate-polyacrylamide gel electrophoresis; FACS, fluorescence activated cell sorting; GGPP, geranylgeranyl diphosphate.

10.1021/jm0701829 CCC: $37.00
Published on Web 06/08/2007

Scheme 2[a]

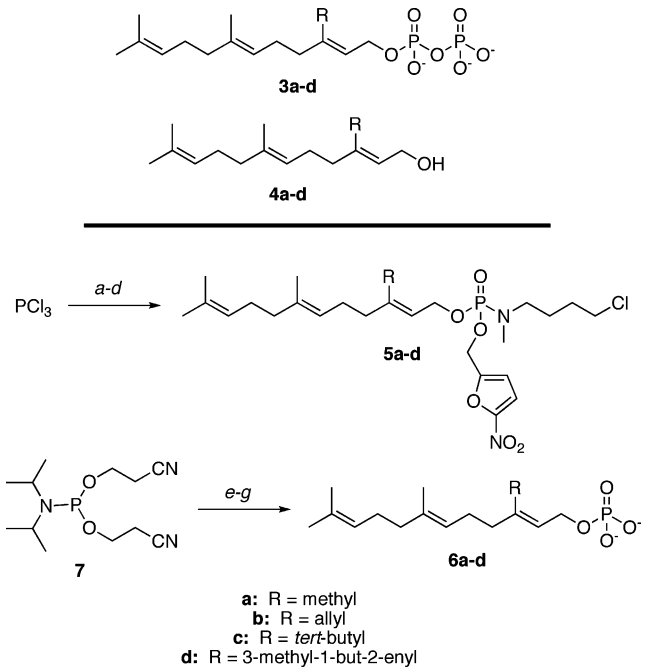

[a] Reagents and conditions: (a) nitrofurfuryl alcohol, Et_3N, CH_2Cl_2, −78 °C, 20 min; (b) $CH_3NH(CH_2)_4Cl$·HCl, Et_3N, CH_2Cl_2, −60 °C, 15 min; (c) **4a**−**d**, Et_3N, CH_2Cl_2, −40 °C, 25 min; (d) *tert*-BuOOH, CH_2Cl_2, −40 to −20 °C, 20 min; (e) **4b**−**d**, tetrazole, THF, 0 °C to rt, 1 h; (f) $NaIO_4$, pyridine, H_2O, 0 °C to rt, 1 h; (g) NaOMe, MeOH, rt, 2 d.

significant advantages over the existing peptide-competitive ones, including synergy with statins (vide infra).[13,15]

A second strategy, to deliver the farnesyl monophosphate derivatives in cells via appropriately masked prodrug precursors, might provide an effective therapeutic approach by one of two mechanisms. First, evidence in both mammalian[16] and plant cells[17] indicates that the diphosphates are generated intracellularly by phosphorylation of the monophosphates. Thus, the intracellular monophosphate of an inhibitor might be converted to the diphosphate within the target cell in a more rapid and effective manner than through the sequential monophosphorylation of the alcohol precursor. Second, the monophosphates themselves might also serve as effective inhibitors of the enzyme. The Borch laboratory has an ongoing interest in the design of prodrugs that utilize phosphoramidate cyclization and cleavage to deliver a variety of different phosphates to tumor cells.[18−20] In this approach, the neutral prodrug enters the cell by passive diffusion, and then intracellular activation of the prodrug generates an intermediate that spontaneously releases the corresponding monophosphate within the cell. This approach has been utilized to enhance the cellular selectivity and efficacy of anticancer nucleoside analogs,[18,19] which also must be converted into the corresponding phosphate derivatives for intracellular activity. We now report the synthesis of phosphoramidate prodrugs of 3-allyl, 3-*tert*-butyl, and 3-(3-methylbut-2-enyl)farnesol (**5b**−**d**) and their biological evaluation versus a human malignant schwannoma cell line (STS-26T), which is not sensitive to treatment with 3-allylfarnesol. We also report the synthesis of the corresponding monophosphates of these three analogs (**6b**−**d**) and the surprising results of their evaluation in vitro as FTase inhibitors.

Results

Prodrug Synthesis. Four novel phosphoramidates (**5a**−**d**) and three novel monophosphates (**6b**−**d**) have been prepared in this initial study. Compound **5a** is the prototype compound prepared from farnesol and, if it were administered, would deliver the natural substrate farnesol monophosphate. Note that **5a** also provides a useful control compound for biological assays (see below). It was used to develop the chemistry required for the synthesis of the three target compounds. Compounds **5b**−**d** are prodrugs that are expected to deliver the corresponding farnesol analog monophosphates **6b**−**d** intracellularly. The farnesol analogs required for the synthesis (**4b**−**d**) were prepared by the methods previously described.[10,21] Initial attempts to prepare the model compound **5a** via the coupling of farnesol with a preformed phosphorus(V) chloride intermediate were unsuccessful. However, synthesis of the prodrugs proceeded smoothly via the one-pot phosphorus(III) route previously established for the synthesis of nucleoside phosphoramidates.[19] As shown in Scheme 2, reaction of PCl_3 with nitrofurfuryl alcohol, followed by *N*-methyl-*N*-(4-chlorobutyl)amine, affords the phosphorus(III) chloride intermediate. This intermediate is not isolated, but is directly coupled with the appropriate alcohol, and the resulting phosphoramidite oxidized to give the desired prodrugs **5a**−**d** in good overall yields (46−62%, based on the starting farnesol analog).

The monophosphates **6b**−**d** are not expected to enter cells readily and, thus, are unlikely to have potent biological activity, but they are important compounds to evaluate as inhibitors of FTase. This would provide another route, in addition to final conversion to the FPP analog, to block farnesylation in cells. Previously we have shown that phosphoramidate constructs such as **5a**−**d** can be used as synthetic precursors of monophosphates via in situ removal of the "delivery" group followed by cyclization of the masking group and hydrolysis.[18,22] However, this did not prove to be an efficient route to **6b**−**d**, although the use of different "delivery" groups on the phosphoramidate oxygen were explored (unpublished results). The synthesis of monophosphates **6b**−**d**, utilizing the procedure of Branch et al.,[23] is outlined in Scheme 2. Briefly, the phosphorylating reagent **7** is coupled with the appropriate farnesol analog in the presence of tetrazole to give the phosphoramidite intermediate, which is oxidized with sodium periodate and then deprotected with base to give the monophosphate. The overall yields for **6b**−**d** in this protocol ranged from 25 to 36%.

Biochemical Evaluation of Farnesyl Monophosphate Analogs. The kinetic constants for the monophosphate analogs were determined following a continuous spectrofluorimetric FTase assay, originally developed by Pompliano et al. and modified by Poulter and co-workers,[24,25] utilizing Dansyl-GCVLS (which mimics the CaaX box of the prototypical FTase substrate H-Ras) as a cosubstrate. As expected, none of the three monophosphate analogs acted as a substrate for FTase. Further analysis determined that two of these compounds were potent inhibitors of the FTase-mediated farnesylation of the Dansyl-GCVLS peptide. In fact, both 3-allyl and 3-*tert*-butylfarnesyl monophosphates **6b** and **6c** were exceptionally potent inhibitors of the enzyme (IC_{50} values of 13 and 16 nM, respectively). These compounds are comparable in potency to 3-isopropenylFPP, the best FPP-based FTase inhibitor previously reported from our laboratory,[11] despite the absence of a terminal diphosphate group. In comparison, 3-allyl and 3-*tert*-butylFPPs (**3b** and **3c**) are less potent inhibitors than the corresponding monophosphates, with IC_{50} values of 189 nM and 31 nM, respectively.[10] In contrast, 3-(3-methybut-2-enyl)farnesyl monophosphate **6d** had little ability to block the farnesylation of Dansyl-GCVLS, with an IC_{50} estimated at ∼5 μM. The corresponding diphosphate (**3d**) is a substrate for FTase, albeit an unusual peptide-

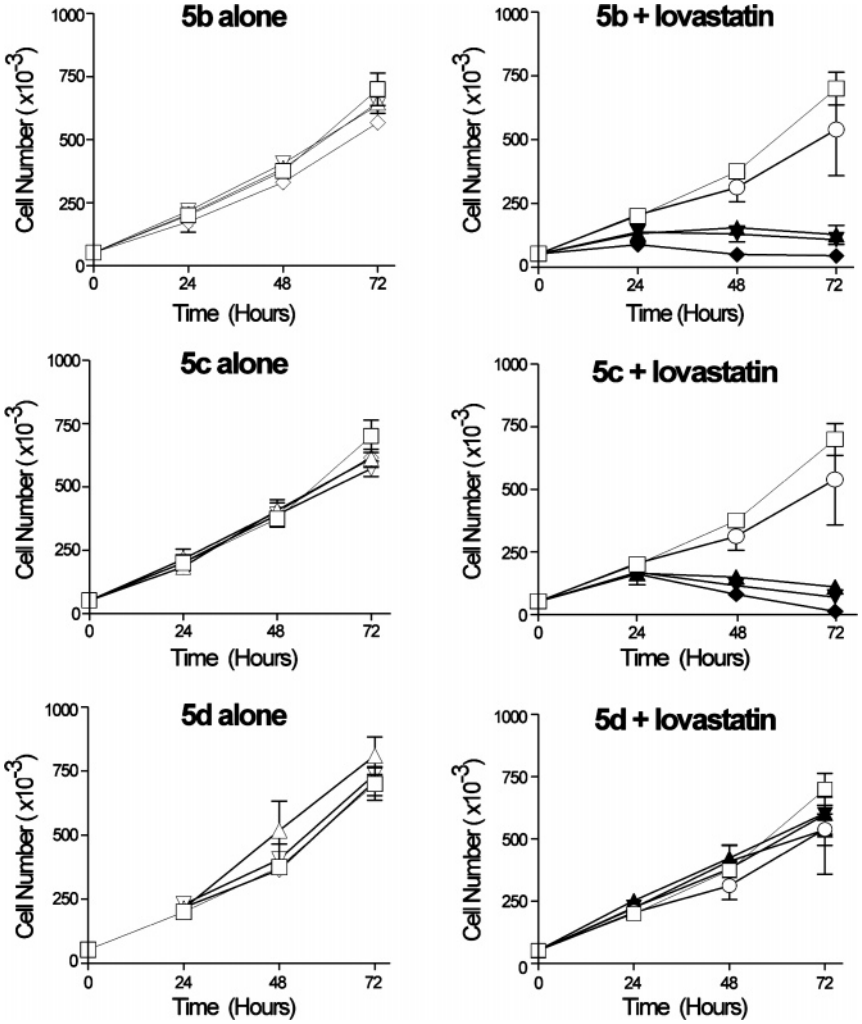

Figure 1. Growth inhibitory effects of **5b**−**d** and lovastatin toward STS-26T cultures. Approximately 24 h after plating, cultures of STS-26T cells were treated singularly with DMSO, **5b**−**d** alone or a combination of **5b**−**d** and lovastatin. Cultures were harvested at various times thereafter for analyses of cell numbers. Data represent means ± SD of three culture dishes. Treatments were as follows: □, DMSO; ○, lovastatin 1 μM; ▲, ▼, ◆, **5b**, **c**, or **d** at 1, 3, or 5 μM (±1 μM lovastatin), respectively.

selective one.[21] It has a K_m value of 800 nM with Dansyl-GCVLS as a cosubstrate. These findings led us to evaluate farnesyl monophosphate itself (**6a**) as an inhibitor of FTase. Under the same conditions used to evaluate **6b**−**d**, it proved to be a more than one order of magnitude less potent than **6b** and **6c**, with an IC_{50} value of ∼210 nM, although its evaluation as an inhibitor is complicated somewhat by its concomitant (but also modest) ability to act as an FTase substrate.[26]

Cellular Evaluation of Farnesyl Phosphate Prodrugs. The effects of prodrugs **5b**−**d** on the proliferation of STS-26T cells were assessed in an in vitro assay; the results are summarized in Figure 1. Growth inhibition was not observed for any of the prodrugs when used alone at 1−5 μM concentrations. However, treatment of cells with **5b** or **5c** (1−5 μM) in combination with 1 μM lovastatin showed almost total growth inhibition at 48 h and cytotoxicity at later time points. In contrast, **5d** was inactive even in the presence of lovastatin. The latter point is important, as **5d** should be significantly less active if its biological activity results from the corresponding monophosphate **6b**, which is a modest FTase inhibitor. This result also provides an important control against the possibility that the biological effects of **5b** or **5c** on STS-26T cells are due to the prodrug moieties themselves.

The cell cycle effects of **5b** were assessed by flow cytometric analysis of cells treated for 24 or 48 h with prodrug **5b** with or without lovastatin; the results are shown in Figure 2. Neither 1 μM lovastatin nor 1 μM **5b** alone altered the progression of STS-26T cells through the cell cycle. However, combined treatment with 1 μM lovastatin and 1 μM **5b** caused a very dramatic accumulation of cells in G_1 after 24 h of drug treatment; no effects on cell cycle progression were noted at 12 h (data not shown). Significant apoptosis (16% of **5b**/lovastatin treated cells) was apparent after 48 h (data not shown).

To confirm that the prodrugs are releasing the monophosphate and targeting the farnesyl transferase enzyme, an in vitro experiment was carried out using compound **5b**, and the results are summarized in Figure 3. STS-26T cells were treated with the indicated concentrations of **5b** for 48 h. The prenylation of RhoB was examined, inasmuch as significant evidence suggests that blocking the farnesylation of RhoB is associated with the cytostatic and cytotoxic effects of other FTase inhibitors. Cell lysates were prepared, separated by SDS-PAGE, and prenylated and unprenylated RhoB were detected by Western blot. The lower band, which is predominant in the absence of drug treatment, is the mature, processed (farnesylated and/or geranylgeranylated) RhoB. The upper band is presumably the unprenylated precursor form of RhoB. Compound **5b** alone at 3 μM has a modest ability to block the prenylation of RhoB, as evidenced by the appearance of an upper unprenylated band. In combination with 1 μM lovastatin, which inhibits synthesis

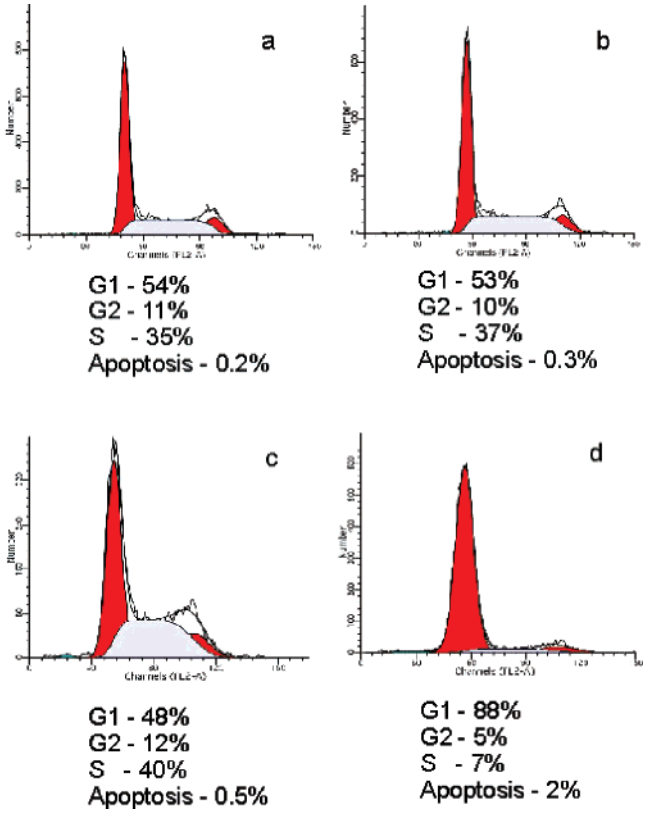

Figure 2. Cell cycle analyses of STS-26T cultures treated with **5b** and lovastatin. Approximately 24 h after plating, STS-26T cultures were treated singularly with (a) DMSO, (b) 1 μM lovastatin alone, (c) 1 μM **5b** alone or (d) a combination of 1 μM **5b** and 1 μM lovastatin. Cultures were harvested 24 h after treatment for analyses of cellular DNA contents by flow cytometry. Actual histograms of 10^4 scored events are presented. MODFIT analyses of a cell cycle phase distribution of nonapoptotic population are noted below individual figures.

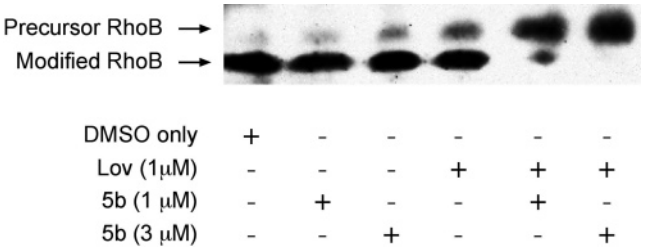

Figure 3. Effect of combination treatment with **5b** and lovastatin on RhoB processing. STS-26T cells were treated for 48 h with the indicated concentrations of **5b** and lovastatin or vehicle control (DMSO) and then whole cell lysates were prepared for western blotting. Immunoblotting for RhoB revealed a mature form of RhoB that was predominant in lysates of control cells (lower arrow). Inhibition of prenylation is revealed by the appearance of the precursor form of RhoB (upper arrow).

of the competing substrates FPP and geranylgeranyl diphosphate, complete inhibition of prenylation is achieved.

The prodrug cellular studies above were performed in combination with 1 μM lovastatin, a level that is achievable in patients[27] but is significantly higher than that typically used in anti-hypercholesterolemic therapy.[28] Therefore, a titration experiment was performed to determine the minimum level of lovastatin required to synergize with 1 μM of the 3-tert-butyl analog **5c**. Strikingly, we have found that even 50 nM lovastatin can lead to a potentiation of the cytostatic effects of **5c**, and 250 nM lovastatin produces an effect essentially equivalent to that seen with 1 μM lovastatin (Figure 4a). Clearly, we see significant effects at lovastatin concentrations that are clinically

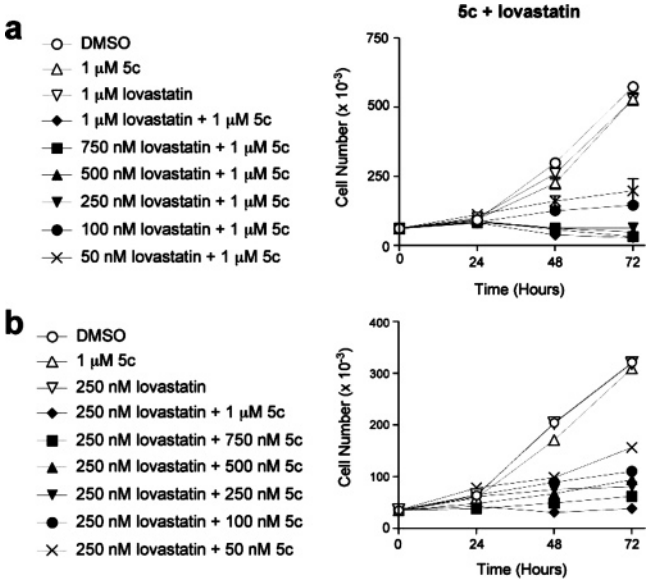

Figure 4. Titration analyses of growth inhibitory effects of varied concentration combinations of **5c** and lovastatin toward STS-26T cultures. Approximately 24 h after plating, cultures of STS-26T cells were treated singularly with (a) DMSO, lovastatin, 1 μM **5c** alone, or a combination of 1 μM **5c** and varying concentrations of lovastatin or (b) DMSO, 1 μM **5c**, 250 nM lovastatin alone, or a combination of 250 nM lovastatin and varying concentrations of **5c**. Cultures were harvested at various times thereafter for analyses of cell numbers. Data represent means $\pm$ SD of three independent experiments (A) or means from two independent experiments.

relevant, and even at a level that is achieved with current clinical antihypercholesterolemic doses of lovastatin.

In a complementary study, we determined the minimum level of **5c** required to synergize with 250 nM lovastatin in the suppression of STS-26T growth. Cultures cotreated with 250 nM lovastatin and concentrations of **5c** ranging from 50−1000 nM exhibited a concentration-dependent suppression of proliferation (Figure 4b). Complete or a near complete suppression of proliferation occurred with concentrations of **5c** $\geq$ 250 nM. Cotreatment with 50 nM **5c** afforded a partial, but significant, suppression of cell growth (Figure 4b).

Discussion. The prodrug strategy employed in this study was motivated by the ineffectiveness of the FPPs versus certain tumor cell lines, including those derived from malignant peripheral nerve sheath tumors, and also by the success of the phosphoramidate prodrug strategy in delivering other phosphate-based enzyme inhibitors. Previously, the Borch laboratory has demonstrated that phosphoramidate prodrug derivatives of nucleoside monophosphates can effectively deliver the nucleotides into tumor cells. Specifically, they have found that this prodrug strategy can be employed for the intracellular delivery of FdUMP[19] and AraCMP.[18] The proposed mechanism of action for the farnesyl phosphoramidates is illustrated in Scheme 3. The 3-allyl phosphoramidate **5b** contains both a "delivery" group (the 2-nitrofuryl moiety) and a "masking" group (the *N*-methyl-*N*-(4-chlorobutyl)amine moiety). The hydrophobic phosphoramidate is taken up by the cell (perhaps through passive diffusion), and the nitrofuryl moiety is reduced to a hydroxylamine that undergoes spontaneous elimination to give intermediate **8**. Activation of the nitrofuryl group may be more rapid in the hypoxic environment of a tumor cell, leading to potential enhanced cellular selectivity of the prodrug. This points out a key advantage of our prodrug strategy over that of Spielmann and coworkers.[29] Cleavage of the nitrofuryl moiety leads to increased reactivity of the masking group, affording cyclization

Scheme 3

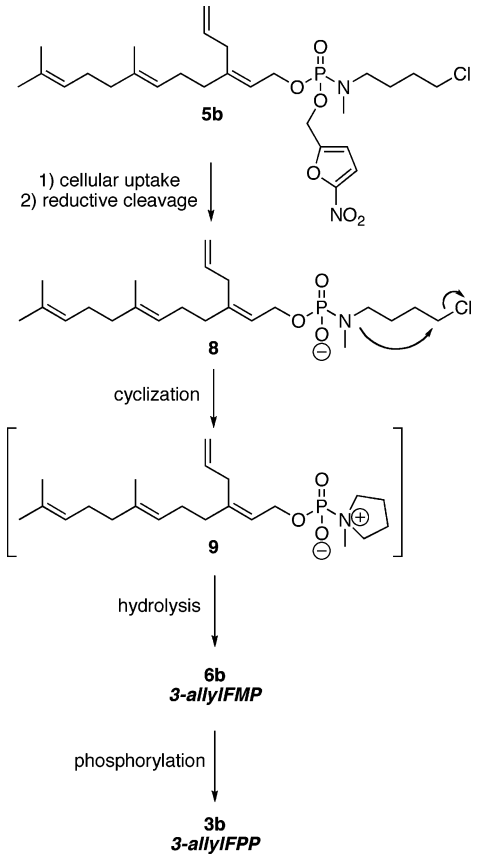

to **9**. This pyrrolidine intermediate then undergoes rapid, spontaneous hydrolysis to 3-allylfarnesyl monophosphate (**6b**). Enzymatic monophosphorylation (by as-yet uncharacterized kinases) would then lead to 3-allylFPP (**3b**), an effective inhibitor of FTase (IC_{50} = 189 nM).[10]

The cellular efficacy of **5b** (and **5c**) is consistent with the mechanism shown in Scheme 3. An alternative mechanism of action for the phosphoramidate prodrug **5b** would involve the direct inhibition of FTase by the monophosphate **6b**. The fact that the parent farnesyl monophosphate binds to FTase argues for the plausibility of this second proposal.[26] Thus, we evaluated the monophosphates **6b**−**d** as potential inhibitors of FTase. It was not surprising that **6b** and **6c** were inhibitors of FTase; however, it was surprising that these compounds were more potent than the corresponding FPP analogs. In fact, the 3-allylfarnesyl monophosphate **6b** (IC_{50} = 13 nM) is more than an order of magnitude more potent than the corresponding diphosphate **4b** (3-allylFPP; IC_{50} = 189 nM). While it is difficult to compare IC_{50} values between different studies, it is clear that **6b** is one of the most potent FPP-based FTase inhibitors yet reported.[5]

The phosphoramidate prodrugs **5b** and **5c** are potent inhibitors of RhoB prenylation and STS-26T proliferation but only in combination with lovastatin. This synergy is consistent with an extensive body of work on the ability of statins to block protein prenylation in cells through inhibition of FPP biosynthesis.[30] Previous studies from our laboratories,[10,13] and from other laboratories,[15] have demonstrated that FPP-competitive FTase inhibitors and statins can synergistically block protein farnesylation. The requirement of both statins and **5b** to effect a blockade of RhoB prenylation reflects the fact that this protein can be either farnesylated or geranylgeranylated. Farnesylation can be blocked by either agent, while geranylgeranylation can only be blocked by statins (assuming that **3b**/**c** or **6b**/**c** cannot block the production of GGPP).

The prenylation of RhoB has been monitored in this study, and the extent of its inhibition is correlated with the extent of cytostasis in STS-26T cells. It is not clear whether or not this indicates that inhibition of RhoB prenylation is a cause of the observed cellular effects in these cells. Prendergast and colleagues have presented evidence that RhoB may be a critical cellular target for FTIs due to a shift in RhoB prenylation toward a geranylgeranylated form that is pro-apoptotic.[31−35] Others, such as the Favre and Sebti groups, demonstrated that both RhoB-F and RhoB-GG inhibit anchorage-dependent and -independent growth, inhibit activation of ERK, and induce apoptosis.[36,37] Thus, while it is an open question as to whether or not RhoB is a target that is responsible for the antitumor effects of FTI treatment, it is clear from a biochemical point of view that it is a good marker for proteins that can be both farnesylated and geranylgeranylated. In particular, it provides a useful test of the ability of our combination treatment of cells with statins and farnesyl monophosphate prodrugs to block prenylation of such proteins.

The statins, hypocholesterolemic agents such as lovastatin that inhibit HMG-CoA reductase, are some of the most widely prescribed drugs in the world and possess a very favorable benefit−risk ratio. Clinical evidence has accumulated over the past several years that the statins have beneficial cardiovascular effects, which are not related to serum cholesterol reduction.[38] Numerous studies have indicated that these "noncholesterol" effects may be due to the inhibition of protein prenylation. It is well-established that treatment of cultured mammalian cells with high levels of statins leads to the inhibition of FPP and GGPP production and, thus, inhibition of protein farnesylation and geranylgeranylation. The common assumption is that cholesterol biosynthesis is much more sensitive to HMG-CoA reductase inhibition than the biosynthesis of dolichol, ubiquinone, or protein prenylation. However, there is an increasing body of both cellular and clinical evidence that statin blockade of HMG-CoA reductase leads to inhibition of protein prenylation, in particular, the protein geranylgeranylation process. Liao and coworkers have demonstrated that stroke protection mediated by statins is due to an increase in endothelial nitric oxide (NO) synthase activity, and this increase can be blocked by cotreatment with GGPP but not FPP.[39] Moreover, this increase in endothelial NO synthase is mediated by Rho family GTPases.[40] Statins are also known to block restenosis, the undesirable and dangerous proliferation of vascular smooth muscle cells seen after angioplasty, and this is also apparently due to a blockage of Rho protein geranylgeranylation.[41] We have reported that the effect of statins on vascular smooth muscle cells is correlated with the inhibition of the prenylation (either farnesylation or geranylgeranylation) of the RhoB protein.[13]

More recent studies have suggested that the statin-mediated blockade of protein prenylation may have an even greater impact on human health than the intriguing cardiovascular results reported above. Some of the most exciting findings have suggested that statins serve as cancer chemoprevention or chemotherapeutic agents. Numerous in vitro studies have indicated that statins are able to block the growth of cultured human tumor cell lines, induce their apoptosis, and block metastasis.[30,42] These studies suggest that these effects also result primarily from the inhibition of protein geranylgeranylation.[43] However, there is a significant amount of controversy about this claim, as it has also been demonstrated that statins can inhibit proteasome-mediated protein degradation, which can lead

to tumor cell apoptosis.[44] Clinical trials evaluating statins as chemotherapeutic agents are ongoing.[30] In phase I studies, it has been demonstrated that lovastatin doses that lead to micromolar bloodstream levels of statins are well-tolerated in patients.[27] While the ability of lovastatin to achieve clinical benefit in cancer patients has not been established, it is clear that levels of the drug that can block protein prenylation (particularly protein geranylgeranylation) in tumor cells can be achieved in vivo, and thus, this ability of statins may be clinically relevant. In summary, it should be noted that a recent review presents the perspective that clinically effective interference with the post-translational modification of signaling proteins such as Ras will require a combination approach with two agents, such as the statin/monophosphate prodrug approach that we have used in this study.[45]

The original FTase inhibitor hypothesis was that FTase inhibitors would suppress cancer cell growth through inhibition of Ras protein action.[46] However, extensive work over the past decade has demonstrated that the link between Ras protein status and FTase inhibitor activity is weak and that inhibition of the prenylation of other proteins[47] may be responsible for the observed anticancer effects. The primary reason for the lack of a correlation of FTase inhibitor activity with Ras status is the alternative geranylgeranylation of N- and K-Ras. The ability of our combined treatment to completely block the prenylation of RhoB (Figure 3) suggests that it may provide an alternative method (rather than the highly toxic FTI/GGTI inhibitors)[48] to block the prenylation of N- and K-Ras and, thus, may be effective against malignant peripheral nerve sheath tumor cells from patients with type 1 neurofibromatosis.[49,50] In summary, it is clear that the combination of lovastatin and prodrug **5b** treatment affords a dramatic cell cycle blockade and, thus, cytostatic effect. The biological and biochemical mechanisms behind this synergistic effect will be explored further in future studies.

Experimental Section

General Synthetic Methods. NMR spectra were recorded on either a Bruker AC 250 MHz or DRX 500 MHz instrument. Proton chemical shifts are reported in parts per million using tetramethylsilane as internal standard. All ^{31}P NMR spectra were acquired using broadband gated decoupling. ^{31}P chemical shifts are reported in parts per million using 0.1% triphenylphosphine oxide in benzene-d_6 as the coaxial reference. Mass spectral data were obtained from the Purdue University Mass Spectrometry Service, and elemental analyses were performed by the Purdue University Microanalysis Lab. Silica gel grade 60 (230−400 mesh) was used to carry out all flash chromatographic separations. Thin layer chromatography was performed using Analtech glass plates precoated with silica gel (250 microns). Visualization of the plates was accomplished using UV and/or the following stains: 1% 4-(*p*-nitrobenzyl)pyridine in acetone followed by heating and subsequent treatment with 3% KOH in methanol; or *p*-anisaldehyde dip (1.85% *p*-anisaldehyde, 20.5% sulfuric acid, and 0.75% acetic acid in 95% ethanol) followed by heating. HPLC analyses were accomplished using a Beckman gradient system (flow rate: 1 mL/min; UV monitoring at 250 nm) and either an Econosphere C_{18} column (5 μm, 4 × 250 mm, Alltech Associates) or a PRP-1 column (7 μm, 4.1 × 250 mm, Hamilton). Preparative HPLC purifications were accomplished using a Rainin Dynamax system equipped with a Hamilton PRP-1 column (12−20 μm, 2.5 × 250 mm, Hamilton) with UV detection at 215 nm and a flow rate of 10 mL/min. Tetrahydrofuran was distilled prior to use from sodium using benzophenone ketyl as an indicator. Dichloromethane, triethylamine, pyridine, and acetonitrile were distilled from calcium hydride prior to use. Unless otherwise noted, all other solvents were purchased from Fisher or VWR and used as received. All chemical reagents were purchased from Aldrich unless otherwise noted.

Synthetic Procedures. (2*E*,6*E*)-3,7,11-Trimethyldodeca-2,6,-10-trien-1-yl 5-Nitrofurfuryl *N*-Methyl-*N*-(4-chlorobutyl) Phosphoramidate (5a). Compound **5a** was prepared using a modified procedure of Meyers et al.[19] 5-Nitrofurfuryl alcohol (200 mg, 1.4 mmol) and *N*-methyl-*N*-(4-chlorobutyl)amine hydrochloride (221 mg, 1.4 mmol) were separately coevaporated three times with 15 mL of anhydrous acetonitrile. Nitrofurfuryl alcohol was then dissolved in 5 mL of dry CH_2Cl_2 and cooled to −78 °C. PCl_3 (0.7 mL, 2.0 M in CH_2Cl_2) was added followed by the dropwise addition of Et_3N (0.43 mL, 3.15 mmol). Stirring was continued at −78 °C for 20 min, and *N*-methyl-*N*-(4-chlorobutyl)amine hydrochloride in 5 mL CH_2Cl_2 was added via cannula followed by dropwise addition of Et_3N (0.87 mL, 6.3 mmol). The reaction mixture was stirred for 15 min, while allowing the temperature to rise from −78 to −60 °C, and the reaction mixture was cannulated to a flask containing *trans*,*trans*-farnesol (**4a**; 0.23 mL, 0.93 mmol) dissolved in 5 mL of CH_2Cl_2 at −40 °C. Et_3N (0.43 mL, 3.15 mmol) was then added dropwise. The reaction proceeded at −40 °C for an additional 20 min. *tert*-Butyl hydroperoxide (0.28 mL, 5.0−6.0 M in decane) was added dropwise to the mixture, and the temperature was raised slowly over 20 min to −20 °C. The reaction mixture was quenched by the addition of saturated NH_4Cl (15 mL) and extracted with 2 × 20 mL of CH_2Cl_2. Column chromatography (1:1 hexanes/ethyl acetate) was performed to yield **5a** as a dark yellow oil (227 mg, 46%). R_f = 0.3 (1:1 hexanes/ethyl acetate). ^{1}H NMR (250 MHz, $CDCl_3$): δ 1.57 (m, 14H), 1.68 (m, 5H), 2.02 (m, 6H), 2.63(d, J = 10 Hz, 3H), 3.04 (m, 2H), 3.55 (m, 2H), 4.49 (t, J = 7.2 Hz, 2H), 4.96 (d, J = 8.8 Hz, 2H), 5.08 (m, 2H), 5.36 (m, 1H) 6.63 (d, J = 3.2 Hz, 1H), 7.27 (s, 1H). ^{31}P NMR ($CDCl_3$): δ −14.2. HPLC 6.18 min, 90.0% (85:15 CH_3CN/0.1% aqueous CF_3CO_2H). HRMS (ESI) calcd for $C_{25}H_{40}ClN_2O_6P$, 553.2210 $(M + Na)^+$; found, 553.2211. Anal. ($C_{25}H_{40}ClN_2O_6P$) C, H, N.

(2*Z*,6*E*)-3-Allyl-7,11-dimethydodeca-2,6,10-trien-1-yl 5-nitrofurfuryl *N*-Methyl-*N*-(4-chlorobutyl) Phosphoramidate (5b). Phosphoramidate **5b** was prepared from 5-nitrofurfuryl alcohol (240 mg, 1.68 mmol), phosphorus trichloride (0.84 mL, 2.0 M in CH_2Cl_2), *N*-methyl-*N*-(4-chlorobutyl)amine hydrochloride (266 mg, 1.68 mmol), (2*Z*,6*E*)-3-allyl-7,11-dimethyldodeca-2,6,10-trien-1-ol (**4b**; 209 mg, 0.84 mmol; prepared as described by Gibbs et al.),[10] and *tert*-butyl hydroperoxide (0.34 mL, 5.0−6.0 M in decane), as described for the above compound **5a**. Column chromatography (2:1 hexanes/ethyl acetate) of the crude product afforded **5b** (251 mg, 54%) as a dark yellow oil. R_f = 0.30 (2:1 hexanes/ethyl acetate). ^{1}H NMR ($CDCl_3$): δ 1.57 (m, 6H), 1.68 (m, 6H), 2.02 (m, 6H), 2.62 (d, J = 10.6 Hz, 3H), 2.83 (d, J = 6.6 Hz, 2H), 3.04 (m, 2H), 3.55 (m, 2H), 4.50 (t, J = 7.1 Hz, 2H), 4.96 (d, J = 8.8 Hz, 2H), 5.05 (m, 2H), 5.43 (m, 1H), 5.71 (m, 1H), 6.63 (d, J = 3.5 Hz, 1H), 7.27 (s, 1H). ^{31}P NMR ($CDCl_3$): δ −14.0. HPLC 8.75 min, 91% (85:15 CH_3CN:0.1% aqueous CF_3CO_2H). HRMS (ESI) calcd for $C_{27}H_{42}ClN_2O_6P$, 557.2574 $(M + H)^+$; found, 557.2565. Anal. ($C_{27}H_{42}ClN_2O_6P$) C, H, N.

(2*Z*,6*E*)-3-*tert*-Butyl-7,11-dimethyldodeca-2,6,10-trien-1-yl 5-nitrofurfuryl *N*-Methyl-*N*-(4-chlorobutyl) Phosphoramidate (5c). Phosphoramidate **5c** was prepared from 5-nitrofurfuryl alcohol (252 mg, 1.76 mmol), phosphorus trichloride (0.88 mL, 2.0 M in CH_2Cl_2), *N*-methyl-*N*-(4-chlorobutyl)amine hydrochloride (278 mg, 1.76 mmol), (2*Z*,6*E*)-3-*tert*-butyl-7,11-dimethyldodeca-2,6,10-trien-1-ol (**4c**; 233 mg, 0.88 mmol; prepared as described by Gibbs et al.),[10] and *tert*-butylhydroperoxide (0.35 mL, 5.0−6.0 M in decane), as described for the above compound **5a**. Column chromatography (2:1 hexanes/ethyl acetate; *p*-anisaldehyde visualization) of the crude product afforded **5c** (279 mg, 55%) as a dark yellow oil. R_f = 0.30 (2:1 hexanes/ethyl acetate). ^{1}H NMR ($CDCl_3$): δ 1.12 (m, 9H), 1.59 (s, 6H), 1.68 (s, 3H), 2.02 (m, 6H), 2.64 (d, J = 10 Hz, 3H), 3.05 (m, 2H), 3.55 (m, 2H), 4.72 (t, J = 6.9 Hz, 2H), 4.97 (d, J = 8.8 Hz, 2H), 5.08 (m, 2H), 5.19 (m, 1H), 6.63 (d, J = 3.2 Hz, 1H), 7.27 (s, 1H). ^{31}P NMR ($CDCl_3$): δ −14.1. HPLC 11.9 min, 91% (85:15 CH_3CN:0.1% aqueous CF_3CO_2H). HRMS (ESI) calcd for $C_{28}H_{46}ClN_2O_6P$, 595.2680 $(M + Na)^+$; found, 595.2692. Anal. ($C_{28}H_{46}ClN_2O_6P$) C, H, N.

(2*Z*,6*E*,10*E*)-3-(3-Methyl-1-but-2-enyl)-7,11-dimethyldodeca-2,6,10-trien-1-yl 5-nitrofurfuryl *N*-Methyl-*N*-(4-chlorobutyl) Phosphoramidate (5d). Phosphoramidate **5d** was prepared from 5-nitrofurfuryl alcohol (175 mg, 1.22 mmol), phosphorus trichloride (0.61 mL, 2.0 M in CH_2Cl_2), *N*-methyl-*N*-(4-chlorobutyl)amine hydrochloride (193 mg, 1.22 mmol), (2*Z*,6*E*)-3-(3-methylbut-2-enyl)-7,11-dimethyldodeca-2,6,10-trien-1-ol (**4d**; 179 mg, 0.61 mmol; prepared as described by Reigard et al.),[21] and *tert*-butylhydroperoxide (0.24 mL, 5.0−6.0 M in decane), as described for the above compound **5a**. Column chromatography (2:1 hexanes/ethyl acetate; *p*-anisaldehyde visualization) of the crude product afforded **5d** (221 mg, 62%) as a dark yellow oil. $R_f = 0.40$ (2:1 hexanes/ethyl acetate). ^{1}H NMR ($CDCl_3$): δ 1.57 (m, 14H), 1.63 (s, 3H), 1.68 (m, 5H), 2.02 (m, 6H), 2.62(d, $J = 10$ Hz, 3H), 2.76 (m, 2H), 3.04 (m, 2H), 3.55 (m, 2H), 4.52 (t, $J = 7.2$ Hz, 2H), 4.96 (d, $J = 8.8$ Hz, 2H), 5.08 (m, 2H), 5.34 (m, 1H), 6.63 (d, $J = 3.2$ Hz, 1H), 7.27 (s, 1H). ^{31}P NMR ($CDCl_3$): δ −14.1. HPLC 7.9 min, 92.6% (85:15 CH_3CN/0.1% aqueous CF_3CO_2H). HRMS (ESI) calcd for $C_{29}H_{46}ClN_2O_6P$, 607.2680 $(M + Na)^+$; found, 607.2687. Anal. ($C_{29}H_{46}ClN_2O_6P$) C, H, N.

(2*Z*,6*E*)-3-*tert*-Butyl-7,11-dimethyldodeca-2,6,10-triene Monophosphate (6c). Bis(2-cyanoethyl)-*N*,*N*-diisopropyl phosphoramidite (**7**; Toronto Research Chemicals, Inc., Canada; 266 mg, 0.98 mmol) and (2*Z*,6*E*)-3-*tert*-butyl-7,11-dimethyldodeca-2,6,10-trien-1-ol (**4c**; 161 mg, 0.61 mmol) were dissolved in 2.8 mL of anhydrous THF and cooled to 0 °C. Sublimed 1*H*-tetrazole (Glen Research, Virginia; 5.2 mL, 0.45 M in acetonitrile) was added to the reaction mixture and stirred for 5 min at 0 °C. The ice bath was removed and stirring was continued at room temperature for 1 h. The reaction mixture was cooled to 0 °C, and pyridine (0.15 mL, 1.83 mmol) was added followed by sodium periodate (2.4 mL, 0.5 M in H_2O). The reaction mixture was stirred for 5 min at 0 °C, and the ice bath was removed. Stirring was continued for 1 h at room temperature. The reaction mixture was diluted with 30 mL of ethyl acetate and poured into 20 mL of saturated sodium sulfite. The sodium sulfite layer was extracted with 30 mL (2×) of ethyl acetate. The combined organic layers were dried over sodium sulfate, and the solvent was removed under reduced pressure to yield the phosphoramidate as a yellow oil. Sodium methoxide (4.14 mL, 0.5 M in MeOH) was added to the oil at room temperature and stirring was continued for 2 days. The solvent was removed from the reaction mixture under reduced pressure to give a yellow residue. The residue was dissolved in a minimal amount of 25 mM NH_4HCO_3 and purified by reversed phase HPLC using a program of 100% A for 5 min followed by a linear gradient of 100% A to 100% B over 30 min (A, 25 mM aqueous NH_4HCO_3; B, CH_3CN; Hamilton PRP-1 21.5 × 250 mm column; flow rate, 10.0 mL/minute; UV monitoring at 215 nm). The fractions were collected, combined, and dried by lyophilization. The white powdery residue was dissolved in 8−10 mL of ion exchange buffer (2:48 v/v isopropyl alcohol/25 mM NH_4HCO_3) and passed through a column containing 50 mL of cation exchange resin (Dowex AG 50W-X8, NH_4^+ form). The column was eluted with two column volumes of ion exchange buffer at a flow rate of 5 mL/min. The eluent was dried by lyophilization to give **6c** (58 mg, 25%) as a white fluffy solid. ^{1}H NMR (CD_3OD): δ 1.12 (s, 9H), 1.59 (s, 6H), 1.65 (s, 3H), 2.08 (m, 8H), 4.63 (m, 2H), 5.11 (m, 2H), 5.30 (m, 1H). ^{31}P NMR (CD_3OD): δ −23.3. HPLC 21.9 min, 90% (100% A for 5 min, 100% A to 100% B over 30 min). HRMS (ESI) calcd for $C_{18}H_{33}O_4P$, 345.2195 $(M + H)^+$; found, 345.2198.

(2*Z*,6*E*)-3-Allyl-7,11-dimethyldodeca-2,6,10-triene Monophosphate (6b). Phosphate **6b** was prepared from bis(2-cyanoethyl)-*N*,*N*-diisopropyl phosphoramidite (**7**; 225 mg, 0.83 mmol), (2*Z*,6*E*)-3-allyl-7,11-dimethyldodeca-2,6,10-trien-1-ol (**4b**; 130 mg, 0.52 mmol), sublimed 1*H*-tetrazole (4.62 mL, 0.45 M in CH_3CN), pyridine (0.13 mL, 1.56 mmol), sodium periodate (2.08 mL, 0.5 M in H_2O), and sodium methoxide (3.5 mL, 0.5 M in MeOH), as described for the above compound **6c**. Column chromatography as described above gave **6b** as a white solid (68 mg, 36%). ^{1}H NMR (CD_3OD): δ 1.59 (s, 6H), 1.65 (s, 3H), 2.08 (m, 8H), 2.86 (d, $J = 6.5$ Hz, 2H), 4.44 (m, 2H), 5.06 (m, 4H), 5.49 (m, 1H), 5.78 (m, 1H). ^{31}P NMR (CD_3OD): δ −24.7. HPLC 20.4 min, 93.1% (100% A for 5 min, 100% A to 100% B over 30 min). HRMS (ESI) calcd for $C_{17}H_{29}O_4P$, 351.1701 $(M + Na)^+$; found, 351.1705.

(2*Z*,6*E*)-3-(3-Methylbut-2-enyl)-7,11-dimethyldodeca-2,6,10-triene Monophosphate (6d). Phosphate **6d** was prepared from bis-(2-cyanoethyl)-*N*,*N*-diisopropyl phosphoramidite (**7**; 68 mg, 0.25 mmol), (2*Z*,6*E*)-3-(3-methylbut-2-enyl)-7,11-dimethyldodeca-2,6,-10-trien-1-ol (**4d**; 72 mg, 0.25 mmol), sublimed tetrazole 1*H*-tetrazole (2.22 mL, 0.45 M in CH_3CN), pyridine (0.06 mL, 0.75 mmol), sodium periodate (1.0 mL, 0.5 M in H_2O), and sodium methoxide (1.70 mL, 0.5 M in MeOH), as described for the above compound **6c**. Column chromatography as described above gave **6d** as a white solid (29 mg, 28% yield). ^{1}H NMR (CD_3OD): δ 1.59 (s, 6H), 1.66 (s, 9H), 2.02 (m, 8H), 2.80 (d, $J = 7.1$ Hz, 2H), 4.46 (m, 2H), 5.07 (m, 3H), 5.40 (m, 1H). ^{31}P NMR (CD_3OD): δ −23.0. HPLC 21.3 min, 93.8% (100% A for 5 min, 100% A to 100% B over 30 min). HRMS (ESI) calcd for $C_{19}H_{33}O_4P$, 379.2014 $(M + Na)^+$; found, 379.2017.

Biochemical Methods. FTase Fluorescent Assay Procedure. The kinetic constants for the FPP analogs were determined following a continuous spectrofluorimetric assay originally developed by Pompliano et al.[24] and modified by Poulter and coworkers.[25] When a dansylated pentapeptide mimicking the CaaX box of human H-Ras as cosubstrate was utilized, the linear portion of the increase in fluorescence versus time was measured with a Spex FluoroMax2 spectrofluorimeter (excitation wavelength = 340 nm; emission wavelength = 500 nm). The assay components [444 μL of assay buffer (52 mM Tris-HCl, pH 7.0, 5.8 mM DTT, 12 mM $MgCl_2$, 12 μM $ZnCl_2$), 6 μL of detergent solution (0.4% *n*-dodecyl-β-D-maltoside in 52 mM Tris-HCl, pH 7.0), 30 μL of peptide solution (12 μM dansyl-GCVLS in 20 mM Tris-HCl, pH 7.0, 10 mM EDTA)] were assembled in a 1.5 mL Eppendorf tube in the order indicated above and were incubated at 30 °C for a period of 5 min. FPP analog or farnesyl monophosphate analog (~10 mM stock solution in 25 mM ammonium bicarbonate, pH 7.5; final concentration 0.10 to 5 μM) was added to the assay solution. The resulting solution was transferred to a 0.75 mL quartz cuvette, the reaction was then initiated with addition of recombinant rat FTase (final concentration in the assay = 0.01 μM; expressed in *E. coli* and purified as described previously by Zimmerman et al.);[51] fluorescence was monitored using a time-based scan at 30 °C for a period of 300 s measuring increase in emission at 500 nm.

Determination of IC_{50} Values for Farnesyl Monophosphate Analog Inhibition of FTase. Initial rates at each indicated monophosphate concentration were determined using the standard fluorescence assay procedure described above, with fixed concentrations of FPP (1.35 μM) and dansyl-GCVLS (0.7 μM). An IC_{50} value of 13 nM for **6b** was estimated from a plot of the velocities versus 3-allylfarnesyl monophosphate concentration (using the program GraphPad Prism 4). In a similar manner, an IC_{50} value of 16 nM was determined for **6c**. The IC_{50} value for **6d** was significantly higher and could not be determined accurately, although a value of 5 μM was estimated from the data plot.

Cellular Biology Methods. Cell Culture and Treatments. The STS-26T cell line was obtained from S. Scoles, Cedars-Sinai Medical Center, Los Angeles, CA. Cells were maintained as adherent cultures at 37 °C, in a humidified incubator with a 5% CO_2 atmosphere, and grown in RPMI-1640 (Gibco) that was supplemented with 5% fetal bovine serum (Hyclone Laboratories, Logan, UT), 100 μg/mL streptomycin, and 100 units/mL penicillin (Invitrogen, Carlsbad, CA). For studies involving drug treatment, cultures were plated in medium containing 5% fetal bovine serum. Cells were released from culture dishes by trypsinization and counted with a hemocytometer. The ability to exclude trypan blue was used as a measurement of viability.

Flow Cytometry. STS-26T cells were harvested and processed for FACs analyses of DNA content as previously described.[47] DNA analyses were made with a BD Biosciences FACS calibur instrument (BD Biosciences). Percentages of cells in the G_1, S, and G_2/M stages of the cell cycle were determined with a DNA histogram-

fitting program (MODFIT; Verity Software). A minimum of 10^4 events/sample was collected for subsequent analyses.

Western Blot Analysis. Primary antibodies used were polyclonal anti-RhoB (Santa Cruz Biotechnology, Santa Cruz, CA) at 1:100. The polyclonal antibody to RhoB can selectively recognize RhoB and not RhoA. Secondary antibodies coupled to horseradish peroxidase (Santa Cruz) were diluted to 1:25 000 and detection was performed with Dura enhanced chemiluminescence reagents (Pierce, Rockford, IL). Data were collected using a Fuji-Film LAS 1000 plus imaging system and exposure to film.

Acknowledgment. This work was supported by the NIH (CA 34619 to R.F.B.; P30 CA21368 (Purdue Cancer Center Support Grant); and P30 ES06639 (Imaging and Cytometry Facility Core of the WSU Toxicology Center Grant)), and by the U.S. Army Neurofibromatosis Research Program (NF020054 to R.R.M.). S.A.S. was supported by a Purdue Research Foundation Fellowship. J.W. was supported by T32 ES012163. We thank Katherine Hicks and Professor Carol A. Fierke (University of Michigan) for supplying the mammalian FTase used to evaluate **6a**−**d** as inhibitors, and CAF for discussions on the ability of **6a** to serve as an FTase substrate. We also thank Michelle Maynor (Purdue) for performing the biochemical evaluation of **6a**.

Supporting Information Available: Table of elemental analyses for compounds **5a**, **5b**, **5c**, and **5d**. This material is available free of charge via the Internet at http://pubs.acs.org.

References

(1) Casey, P. J.; Seabra, M. C. Protein Prenyltransferases. *J. Biol. Chem.* **1996**, *271*, 5289−5292.
(2) Zhang, F. L.; Casey, P. J. Protein Prenylation: Molecular Mechanisms and Functional Consequences. *Annu. Rev. Biochem.* **1996**, *65*, 241−269.
(3) McTaggart, S. J. Isoprenylated Proteins. *Cell. Mol. Life Sci.* **2006**, *63*, 255−267.
(4) Downward, J. Targeting Ras Signalling Pathways in Cancer Therapy. *Nat. Rev. Cancer* **2002**, *3*, 11−22.
(5) Gibbs, R. A.; Zahn, T. J.; Sebolt-Leopold, J. S. Non-Peptidic Prenyltransferase Inhibitors: Diverse Structural Classes and Surprising Anti-Cancer Mechanisms. *Curr. Med. Chem.* **2001**, *8*, 1437−1466.
(6) Bell, I. M. Inhibitors of Farnesyltransferase: A Rational Approach to Cancer Chemotherapy? *J. Med. Chem.* **2004**, 47, 1869−1878.
(7) Zujewski, J.; Horak, I. D.; Bol, C. J.; Woestenborghs, R.; Bowden, C.; End, D. W.; Piotrovsky, V. K.; Chiao, J.; Belly, R. T.; Todd, A.; Kopp, W. C.; Kohler, D. R.; Chow, C.; Noone, M.; Hakim, F. T.; Larkin, G.; Gress, R. E.; Nussenblatt, R. B.; Kremer, A. B.; Cowan, K. H. Phase I and Pharmacokinetic Study of Farnesyl Protein Transferase Inhibitor R115777 in Advanced Cancer. *J. Clin. Oncol.* **2000**, *18*, 927−941.
(8) Njorge, F. G.; Taveras, A. G.; Kelly, J.; Remiszewski, S.; Mallamas, A. K.; Wolin, R.; Afonso, A.; Cooper, A. B.; Rane, D. F.; Liu, Y. T.; Wong, J.; Vibulbhan, B.; Pinto, P.; Deskus, J.; Alvarez, C. S.; delRosario, J.; Connolly, M.; Wang, J.; Desai, J.; Rossman, R. R.; Bishop, W. R.; Patton, R.; Wang, L.; Kirschmeier, P.; Bryant, M. S.; Nomeir, A. A.; Lin, C. C.; Liu, M.; McPhail, A. T.; Doll, R. J.; Girijavallabhan, V. M.; Ganguly, A. K. (+)-4-[2-[4-(8-Chloro-3,10-dibromo-6,11-dihydro-5*H*-benzo[5,6]cyclohepta[1,2-*b*]pyridini-11(*R*)-1-piperidinecarboxyamide (SCH-66336): A Very Potent Farnesyl Protein Transferase Inhibitor as a Novel Antitumor Agent. *J. Med. Chem.* **1998**, *41*, 4890−4902.
(9) Basso, A. D.; Kirschmeier, P. T.; Bishop, W. R. Farnesyl Transferase Inhibitors. *J. Lipid Res.* **2006**, *47*, 15−31.
(10) Gibbs, B. S.; Zahn, T. J.; Mu, Y. Q.; Sebolt-Leopold, J.; Gibbs, R. A. Novel Farnesol and Geranylgeraniol Analogues: A Potential New Class of Anticancer Agents Directed against Protein Prenylation. *J. Med. Chem.* **1999**, *42*, 3800−3808.
(11) Zahn, T. J.; Weinbaum, C.; Gibbs, R. A. Grignard-Mediated Synthesis and Preliminary Biological Evaluation of Novel 3-Substituted Farnesyl Diphosphate Analogues. *Bioorg. Med. Chem. Lett.* **2000**, *10*, 1763−1766.
(12) Crick, D. C.; Andres, D. A.; Waecheter, C. J. Novel Salvage Pathway Utilizing Farnesol and Geranylgeraniol for Protein Isoprenylation. *Biochem. Biophys. Res. Commun.* **1997**, *237*, 483−487.
(13) Mattingly, R. R.; Gibbs, R. A.; Menard, R. E.; Reiners, J. J. Potent Suppresion of the Proliferation of A10 Vascular Smooth Muscle Cells by Combined Treatment with 3-Allylfarnesol, an Inhibitor of Protein Farnesyltransferase. *J. Pharm. Exp. Ther.* **2002**, *303*, 74−81.
(14) Amin, R.; Chen, H. Q.; Tannous, M.; Gibbs, R.; Kowluru, A. Inhibition of Glucose- and Calcium-Induced Insulin Secretion from βTC3 Cells by Novel Inhibitors of Protein Isoprenylation. *J. Pharm. Exp. Ther.* **2002**, *303*, 82−88.
(15) Yonemoto, M.; Satoh, T.; Arakawa, H.; Suzuki-Takahashi, I.; Monden, Y.; Kodera, T.; Tanaka, K.; Aoyama, T.; Iwasawa, Y.; Kamei, T.; Nishimura, S.; Tomimoto, K. J-104,871, a Novel Farnesyltransferase Inhibitor, Blocks Ras Farnesylation in a Farnesyl Pyrophosphate-Competitive Manner. *Mol. Pharm.* **1998**, *54*, 1−7.
(16) Bentinger, M.; Grunler, J.; Peterson, E.; Swiezewska, E.; Dallner, G. Phosphorylation of Farnesol in Rat Liver Microsomes: Properties of Farnesol Kinase and Farnesyl Phosphate Kinase. *Arch. Biochem. Biophys.* **1998**, *353*, 191−198.
(17) Thai, L.; Rush, J. S.; Maul, J. E.; Devarenne, T.; Rodgers, D. L.; Chappell, J.; Waechter, C. J. Farnesol Is Utilized for Isoprenoid Biosynthesis in Plant Cells via Farnesyl Pyrophosphate Formed by Successive Monophosphorylation Reactions. *Proc. Natl. Acad. Sci. U.S.A.* **1999**, *96*, 13080−13085.
(18) Tobias, S. C.; Borch, R. F. Synthesis and Biological Studies of Novel Nucleoside Phosphoramidate Prodrugs. *J. Med. Chem.* **2001**, *44*, 4475−4480.
(19) Meyers, C. L. F.; Hong, L.; Joswig, C.; Borch, R. F. Synthesis and Biological Activity of Novel 5-Fluoro-2′-deoxyuridine Phosphoramidate Prodrugs. *J. Med. Chem.* **2000**, *43*, 4313−4318.
(20) Borch, R. F.; Liu, J.; Schmnidt, J. P.; Marakovits, J. T.; Joswig, C.; Gipp, J. J.; Mulcahy, R. T. Synthesis and Evaluation of Nitroheterocyclic Phosphoramidates as Hypoxia-Selective Alkylating Agents. *J. Med. Chem.* **2000**, *43*, 2258−2265.
(21) Reigard, S. A.; Zahn, T. J.; Haworth, K. B.; Hicks, K. A.; Fierke, C. A.; Gibbs, R. A. Interplay of Isoprenoid and Peptide Substrate Specificity in Protein Farnesyltransferase. *Biochemistry* **2005**, *44*, 11214−11223.
(22) Wu, W.; Meyers, C. L. F.; Borch, R. F. A Novel Method for the Preparation of Nucleoside Triphosphates from Activated Nucleoside Phosphoramidates. *Org. Lett.* **2004**, *6*, 2257−2260.
(23) Branch, C. L.; Burton, G.; Moss, S. F. An Expedient Synthesis of Allylic Polyprenol Phosphates. *Synth. Commun.* **1999**, *29*, 2639−2644.
(24) Pompliano, D. L.; Gomez, R. P.; Anthony, N. J. Intramolecular Fluorescence Enhancement: A Continuous Assay of Ras Farnesyl/Protein Transferase. *J. Am. Chem. Soc.* **1992**, *114*, 7945−7946.
(25) Cassidy, P. B.; Dolence, J. M.; Poulter, C. D. Continuous Fluorescence Assay for Protein Prenyltransferases. *Methods Enzymol.* **1995**, *250*, 30−43.
(26) Saderholm, M. J.; Hightower, K. E.; Fierke, C. A. Role of Metals in the Reaction Catalyzed by Protein Farnesyltransferase. *Biochemistry* **2000**, *39*, 12398−12405.
(27) Holstein, S. A.; Knapp, H. R.; Clamon, G. H.; Murry, D. J.; Hohl, R. J. Pharmacodynamic Effects of High Dose Lovastatin in Subjects with Advanced Malignancies. *Cancer Chemother. Pharmacol.* **2006**, *57*, 155−164.
(28) Pan, H. Y.; DeVault, A. R.; Wang-Iverson, D.; Ivashkiv, E.; Swanson, B. N.; Sugerman, A. A. Comparative Pharmacokinetics and Pharmacodynamics of Pravastatin and Lovastatin. *J. Clin. Pharmacol.* **1990**, *30*, 1128−1135.
(29) Troutman, J. M.; Chehade, K. A. H.; Kiegiel, K.; Andres, D. A.; Spielmann, H. P. Synthesis of Acyloxymethyl Ester Prodrugs of the Transferable Protein Farnesyl Transferase Substrate Farnesyl Methylenediphosphonate. *Bioorg. Med. Chem. Lett.* **2004**, *14*, 4979−4982.
(30) Graaf, M. R.; Richel, D. J.; Noorden, C. J. F. v.; Guchelaar, H.-J. Effects of Statins and Farnesyltransferase Inhibitors on the Development and Progression of Cancer. *Cancer Treat. Rev.* **2004**, *30*, 609−641.
(31) Lebowitz, P. F.; Casey, P. J.; Prendergast, G. C.; Thissen, J. A. Farnesyltransferase Inhibitors Alter the Prenylation and Growth-Stimulating Function of RhoB. *J. Biol. Chem.* **1997**, *272*, 15591−15594.
(32) Du, W.; Lebowitz, P. F.; Prendergast, G. C. Cell Growth Inhibition by Farnesyltransferase Inhibitors Is Mediated by Gain of Geranylgeranylated RhoB. *Mol. Cell. Biol.* **1999**, *19*, 1831−1840.
(33) Prendergast, G. C. Farnesyltransferase Inhibitors: Antineoplastic Mechanism and Clinical Prospects. *Curr. Opin. Cell. Biol.* **2000**, *12*, 166−173.
(34) Du, W.; Prendergast, G. C. Geranylgeranylated RhoB Mediates Suppression of Human Tumor Cell Growth by Farnesyltransferase Inhibitors. *Cancer Res.* **1999**, *59*, 5492−5496.

(35) Liu, A.; Du, W.; Liu, J. P.; Jessell, T. M.; Prendergast, G. C. RhoB Alteration is Necessary for Apoptotic and Antineoplastic Responses to Farnesyltransferase Inhibitors. *Mol. Cell. Biol.* **2000**, *20*, 6105−6113.
(36) Chen, Z.; Otto, J. C.; Bergo, M. O.; Young, S. G.; Casey, P. J. The C-Terminal Polylysine Region and Methylation of K-Ras Are Critical for the Interaction between K-Ras and Microtubules. *J. Biol. Chem.* **2000**, *275*, 41251−41257.
(37) Mazieres, J.; Tillement, V.; Allal, C.; Clanet, C.; Bobin, L.; Chen, Z.; Sebti, S. M.; Favre, G.; Pradines, A. Geranylgeranylated, but not Farnesylated, RhoB Suppresses Ras Transformation of NIH-3T3 Cells. *Exp. Cell Res.* **2005**, *304*, 354−364.
(38) Massy, Z. A.; Keane, W. F.; Kasiske, B. L. Inhibition of the Mevalonate Pathway: Benefits Beyond Cholesterol Reduction? *Lancet* **1996**, *347*, 102−103.
(39) Endres, M.; Laufs, U.; Huang, Z.; nakamura, T.; Huang, P.; Moskowitz, M. A.; Liao, J. K. Stroke Protection by 3-Hydroxy-3-methylglutaryl (HMG)-CoA Reductase Inhibitors Mediated by Endothelial Nitric Oxide Synthase. *Proc. Natl. Acad. Sci. U.S.A.* **1998**, *95*, 8880−8885.
(40) Laufs, U.; Liao, J. K. Post-Transcriptional Regulation of Endothelial Nitric Oxide Synthase mRNA Stability by Rho GTPase. *J. Biol. Chem.* **1998**, *273*, 24266−24271.
(41) Laufs, U.; Marra, D.; Node, K.; Liao, J. K. 3-Hydroxy-3-methylglutaryl-CoA Reductase Inhibitors Attenuate Vascular Smooth Muscle Proliferation by Preventing Rho GTPase-Induced Down-Regulation of p27Kip1. *J. Biol. Chem.* **1999**, *274*, 21926−21931.
(42) Chan, K. K. W.; Oza, A. M.; Siu, L. L. The Statins as Anticancer Agents. *Clin. Cancer Res.* **2003**, *9*, 10−19.
(43) McGuire, T. F.; Sebti, S. M. Geranylgeraniol Potentiates Lovastatin Inhibition of Oncogenic H-Ras Processing and Signaling while Preventing Cytotoxicity. *Oncogene* **1997**, *12*, 305−312.
(44) Brower, V. Of Cancer and Cholesterol: Studies Elucidate Anticancer Mechanism of Statin. *J. Natl. Cancer. Inst.* **2003**, *95*, 844−846.
(45) Konstantinopoulos, P. A.; Papavassiliou, A. T. Multilevel Modulation of the Mevalonate and Protein-−Prenylation Circuitries as a Novel Strategy for Anticancer Therapy. *Trends Pharmacol. Sci.* **2007**, *28*, 6−13.
(46) Gibbs, J. B. Ras C-Terminal Processing Enzymes−New Drug Targets? *Cell* **1991**, *65*, 1−4.
(47) Cox, A. D.; Der, C. J. Farnesyltransferase Inhibitors and Cancer Treatment: Targeting Simply Ras? *Biochem. Biophys. Acta* **1997**, *1333*, F51−F71.
(48) deSolms, S. J.; Ciccarone, T. M.; MacTough, S. C.; Shaw, A. W.; Buser, C. A.; Ellis-Hutchings, M.; Fernandes, C.; Hamilton, K. A.; Huber, H. E.; Kohl, N. E.; Lobell, R. B.; Robinson, R. G.; Tsou, N. N.; Walsh, E. S.; Graham, S. L.; Beese, L. S.; Taylor, J. S. Dual Protein Farnesyltransferase-Geranylgeranyltransferase I Inhibitors as Potential Cancer Chemotherapeutic Agents. *J. Med. Chem.* **2003**, *46*, 2973−2984.
(49) Mattingly, R. R.; Kraniak, J. M.; Dilworth, J. T.; Mathieu, P.; Bealmear, B.; Nowak, J. E.; Benjamins, J. A.; Tainsky, M. A.; Reiners, J. J. The Mitogen-Activated Protein Kinase/Extracellular Signal-Regulated Kinase Inhibitor PD184352 (CI-1040) Selectively Induces Apoptosis in Malignant Schwannoma Cell Lines. *J. Pharm. Exp. Ther.* **2006**, *316*, 456−465.
(50) Dilworth, J. T.; Kraniak, J. M.; Woitkowiak, J. W.; Gibbs, R. A.; Borch, R. F.; Tainsky, M. A.; Reiners, J. J.; Mattingly, R. R. Molecular Targets for Emerging Antitumor Therapies for Neurofibromatosis Type 1. *Biochem. Pharm.* **2006**, *72*, 1485−1492.
(51) Zimmerman, K. K.; Scholten, J. D.; Huang, C. c.; Fierke, C. A.; Hupe, D. J. High-Level Expression of Rat Farnesyl/Protein Transferase in *Escherichia coli* as a Translationally Coupled Heterodimer. *Protein Exp. Purif.* **1998**, *14*, 395−402.

JM0701829